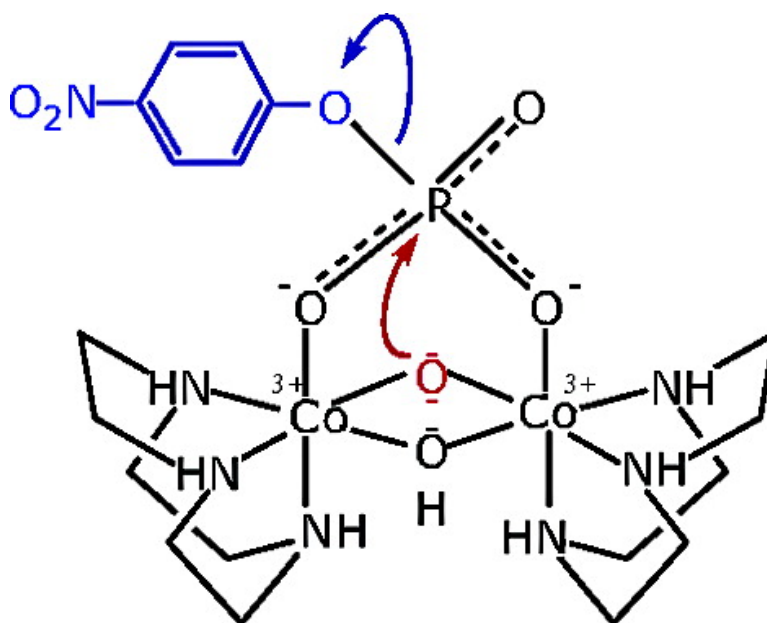


Altered Mechanisms of Reactions of Phosphate Esters Bridging a Dinuclear Metal Center

Tim Humphry, Marcello Forconi, Nicholas H. Williams, and Alvan C. Hengge

J. Am. Chem. Soc., **2004**, 126 (38), 11864-11869 • DOI: 10.1021/ja047110g • Publication Date (Web): 04 September 2004

Downloaded from <http://pubs.acs.org> on April 1, 2009



More About This Article

Additional resources and features associated with this article are available within the HTML version:

- Supporting Information
- Links to the 3 articles that cite this article, as of the time of this article download
- Access to high resolution figures
- Links to articles and content related to this article
- Copyright permission to reproduce figures and/or text from this article

[View the Full Text HTML](#)



ACS Publications
 High quality. High impact.

Altered Mechanisms of Reactions of Phosphate Esters Bridging a Dinuclear Metal Center

Tim Humphry,[†] Marcello Forconi,[‡] Nicholas H. Williams,^{*,‡} and Alvan C. Hengge^{*,†}

Contribution from the Department of Chemistry and Biochemistry, Utah State University, Logan, Utah 84322-0300, and Department of Chemistry, University of Sheffield, Sheffield, U.K. S3 7HF

Received May 17, 2004; E-mail: N.H.Williams@sheffield.ac.uk; hengge@cc.usu.edu

Abstract: Kinetic isotope effects in the nucleophile and leaving group were obtained for the reaction of *p*-nitrophenyl phosphate monoester coordinated to a dinuclear Co(III) complex. The metal complex of the *p*-nitrophenyl phosphate monoester was found to hydrolyze by a single-step concerted mechanism, with significant nucleophilic participation in the transition state. By contrast, the hydrolysis of uncomplexed *p*-nitrophenyl phosphate occurs by a very loose transition state with little bond formation to the nucleophile. Previously, the metal complex of the diester methyl-*p*-nitrophenyl phosphate was found to hydrolyze via a two-step addition–elimination mechanism, in contrast to the concerted hydrolysis mechanism followed by uncomplexed diesters with the *p*-nitrophenolate leaving group. These results show that coordination to a metal complex can significantly alter the mechanism of phosphoryl transfer.

Introduction

Phosphate esters are cleaved in biological systems by two classes of phosphatases that act by different mechanisms. One, exemplified by alkaline phosphatases and protein–tyrosine phosphatases, uses an enzymatic nucleophile to form a phosphoenzyme intermediate that is subsequently cleaved by water. A second group catalyzes direct phosphoryl transfer to a metal-coordinated water molecule. The latter are typified by the “diamond core” phosphatases, a superfamily of metallophosphatases that contain a dinuclear metal center motif (Figure 1). Some diamond core phosphatases whose X-ray structures have been reported include protein phosphatase 1 (PP-1), protein phosphatase 2B (calcineurin- α or PP-2B), λ protein phosphatase (λ PP), and the purple acid phosphatases, such as that from kidney bean (KBPAP).^{1,2}

Figure 1 is a comparison of the active site of KBPAP with a *p*NPP coordinated to a dicobalt complex that has been shown to greatly accelerate the reactions of both coordinated phosphodiester and monoesters. For *p*NPP, coordination provides a rate enhancement of $\sim 10^{12}$.³ For the diester methyl *p*-nitrophenyl phosphate, the acceleration is $\sim 10^{10}$.⁴ The metal–metal distance in the model complex is very similar to the

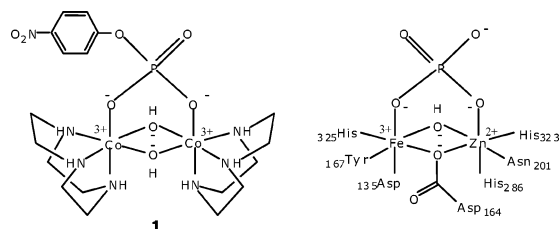


Figure 1. Comparison of the cationic portion of monoester complex **1** with the active site of PAP.

analogous distance in the enzyme (2.9 vs 3.1 Å).^{1,3} Labeling studies using ¹⁸O have revealed that the model complex uses one of the bridging oxygen atoms as a nucleophile.³ The bridging hydroxide ion has also been suggested as the nucleophile in diamond core phosphatases.^{1,5}

The role of metal ions in catalysis of phosphoryl transfer reactions has been considered in numerous reviews.⁶ One central issue is whether metal ions change the nature of the phosphoryl transfer step itself. Phosphoryl transfer may proceed by transition states that are very loose, in which bond fission exceeds bond formation to the nucleophile, or tight, in which the transition state resembles a pentacoordinate phosphorane.

Phosphate Ester Hydrolysis. Figure 2 depicts a More-O’Ferrall–Jencks diagram for phosphate ester hydrolysis. The two-step mechanisms A ($A_N + D_N$ with a phosphorane intermediate) and B ($D_N + A_N$ with a metaphosphate intermediate) proceed via the upper left and lower right corners,

[†] Utah State University.

[‡] University of Sheffield.

- (1) Strater, N.; Klabunde, T.; Tucker, P.; Witzel, H.; Krebs, B. *Science* **1995**, *268*, 1489–1492.
- (2) Kissinger, C. R.; Parge, H. E.; Knighton, D. R.; Lewis, C. T.; Pelletier, L. A.; Tempczyk, A.; Kalish, V. J.; Tucker, K. D.; Showalter, R. E.; Moomaw, E. W. *Nature* **1995**, *378*, 641–644. Klabunde, T.; Strater, N.; Frohlich, R.; Witzel, H.; Krebs, B. *J. Mol. Biol.* **1996**, *259*, 737–748. Goldberg, J.; Huang, H. B.; Kwon, Y. G.; Greengard, P.; Nairn, A. C.; Kuriyan, J. *Nature* **1995**, *376*, 745–753. Egloff, M.; Cohen, P. T.; Reinemer, P.; Barford, D. *J. Mol. Biol.* **1995**, *254*, 942–959.
- (3) Williams, N. H.; Lebus, A.-M.; Chin, J. *J. Am. Chem. Soc.* **1999**, *121*, 3341–3348.
- (4) Williams, N. H.; Cheung, W.; Chin, J. *J. Am. Chem. Soc.* **1998**, *120*, 8079–8087.

- (5) Smoukov, S. K.; Quaroni, L.; Wang, X.; Doan, P. E.; Hoffman, B. M.; Que, L., Jr. *J. Am. Chem. Soc.* **2002**, *124*, 2595–2603.
- (6) Strater, N.; Lipscomb, W. N.; Klabunde, T.; Krebs, B. *Angew. Chem., Intl. Ed. Engl.* **1996**, *35*, 2024–2055. Williams, N. H.; Takasaki, B.; Wall, M.; Chin, J. *Acc. Chem. Res.* **1999**, *32*, 485–493. Hendry, P.; Sargeson, A. M. *Prog. Inorg. Chem.* **1990**, *38*, 201–258. Vichard, C.; Kaden, T. A. *Inorg. Chim. Acta* **2002**, *337*, 173–180.

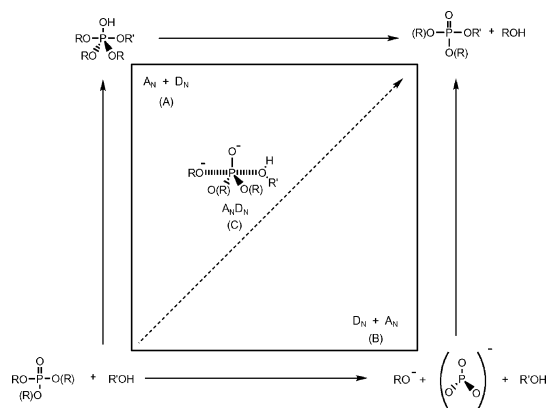


Figure 2. A More-O'Ferrall–Jencks diagram illustrating the range of pathways possible for phosphate ester hydrolysis.

respectively. The reactions of the dianions of phosphate monoesters are concerted ($A_N D_N$), albeit with loose transition states that lie in the lower right-hand region of the diagram.⁷ For reactions of monoanions, metaphosphate has not been ruled out, but stereochemical studies⁸ showing that the reaction proceeds by inversion imply that, if metaphosphate forms, it is a fleeting intermediate in a preassociative mechanism. Whether such an intermediate forms or not, the transition state is loose, as in the dianion reaction.

Phosphodiester with aryl leaving groups have been shown by linear free energy relationships⁹ and kinetic isotope effects^{10,11} to also react by a concerted pathway, although the transition state is tighter, in the central region of the diagram of Figure 2. Phosphotriesters react by concerted mechanisms with tight transition states (upper left region of the More-O'Ferrall–Jencks diagram) or in some cases, such as with cyclic triesters or under acidic conditions, form phosphorane intermediates. It has been pointed out that a common thread in this mechanistic continuum is that the phosphoryl group appears to maintain a charge of -1 in the transition state.¹²

In a tight transition state, negative charge on the phosphoryl group increases. Thus interactions with metal ions or positively charged amino acids intuitively would seem to favor an associative mechanism. This simple approach neglects the influence of geometrical differences in the phosphoryl group in the ground state and transition state, which have been shown to have the potential to result in preferential enzymatic stabilization of a loose, metaphosphate-like transition state.¹³ Further, it has been shown that magnesium or calcium ions do not alter the loose transition states for the hydrolysis of aryl phosphate monoesters¹⁴ or of ATP.¹⁵

- (7) Herschlag, D.; Jencks, W. P. *J. Am. Chem. Soc.* **1989**, *111*, 7579–7586. Thatcher, G. R. J.; Kluger, R. *Adv. Phys. Org. Chem.* **1989**, *25*, 99–265. Hengge, A. C. In *Comprehensive Biological Catalysis: A Mechanistic Reference*; Sinnott, M., Ed.; Academic Press: San Diego, CA, 1998; Vol. 1, pp 517–542.
- (8) Buchwald, S. L.; Friedman, J. M.; Knowles, J. R. *J. Am. Chem. Soc.* **1984**, *106*, 4911–4916.
- (9) Ba-Saif, S. A.; Davis, A. M.; Williams, A. *J. Org. Chem.* **1989**, *54*, 5483–5486. Kirby, A. J.; Younas, M. *J. Chem. Soc. (B)* **1970**, 1165–1172.
- (10) Cassano, A. G.; Anderson, V. E.; Harris, M. E. *J. Am. Chem. Soc.* **2002**, *124*, 10964–10965.
- (11) Hengge, A. C.; Tobin, A. E.; Cleland, W. W. *J. Am. Chem. Soc.* **1995**, *117*, 5919–5926.
- (12) Cleland, W. W. *FASEB J.* **1990**, *4*, 2899–2905.
- (13) Alhambra, C.; Wu, L.; Zhang, Z.-Y.; Gao, J. *J. Am. Chem. Soc.* **1998**, *120*, 3858–3866. Asthagiri, D.; Dillet, V.; Liu, T.; Noodleman, L.; Van Etten, R. L.; Bashford, D. *J. Am. Chem. Soc.* **2002**, *124*, 10225–10235.
- (14) Herschlag, D.; Jencks, W. P. *J. Am. Chem. Soc.* **1987**, *109*, 4665–4674.
- (15) Admiraal, S. J.; Herschlag, D. *Chem., Biol.* **1995**, *2*, 729–739.

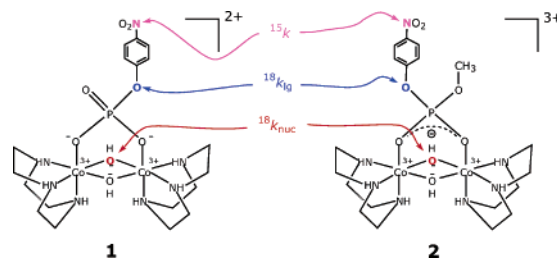


Figure 3. Model complex with monoester substrate (**1**) and diester substrate (**2**). Isotope effects were measured at the positions indicated.

In this study, we report measurements of kinetic isotope effects (KIEs) on the intramolecular reaction of monoester complex **1** and compare the mechanism and transition state of this reaction with an earlier examination¹⁶ of the diester complex **2** (Figure 3). The reaction of the coordinated diester was shown to occur by a two-step addition–elimination ($A_N + D_N$) reaction, in contrast to the concerted phosphoryl transfer mechanism followed by the uncatalyzed hydrolysis of diesters with the same leaving group. The study reported here was intended to ascertain whether a similar change in mechanism, or transition state, in the reaction of the *p*NPP monoester occurs as a result of coordination to the complex.

Isotope Effects. Figure 3 shows the positions at which the isotope effects were measured in the reactions of **1** and **2**. The magnitude of ^{15}k depends on the amount of negative charge developed on the leaving group in the transition state, and arises from contributions of a quinonoid resonance structure in the delocalized nitrophenolate anion. Thus, the EIE for deprotonation of *p*-nitrophenol is normal, 1.0023.¹⁷ The leaving group ^{18}O KIE ($^{18}k_{\text{lg}}$) is a measure of P–O bond fission. The more normal this isotope effect, the weaker (more broken) the bond to the leaving group in the transition state. The nucleophile ^{18}O KIE ($^{18}k_{\text{nuc}}$) is a measure of the degree of bond formation to the nucleophile. Nucleophile KIEs are large and normal for early transition states, when the imaginary frequency factor dominates, and become smaller as the degree of bond formation in the transition state increases, raising the importance of the zero-point energy factor, as discussed below.

Experimental Section

Synthesis of Isotopically Labeled Compounds. Natural abundance *p*-nitrophenyl phosphate, [^{14}N]-*p*-nitrophenyl phosphate, and [^{15}N]-*p*-nitrophenyl phosphate were synthesized as previously described.¹⁸ The ^{15}N isotope effect was measured using complex prepared from natural abundance *p*-NPP as previously described.⁴ The ^{18}O isotope effects were measured using the remote label method, using the nitrogen atom in nitrophenol as a reporter for oxygen isotope ratios.^{19,20} Thus, [^{14}N]-*p*-nitrophenol and [^{15}N]-*p*-nitrophenol- ^{18}O were synthesized¹⁸ and then mixed to closely reconstitute the 0.365% natural abundance of ^{15}N . This mixture was then phosphorylated¹⁸ to produce *p*-nitrophenyl phosphate as a mixture of isotopomers. This mixture was used to prepare the complex⁴ which was then used for determination of the $^{18}\text{O}_{\text{lg}}$ isotope effect.

The nucleophile ^{18}O isotope effect ($^{18}k_{\text{nuc}}$) was measured using complex prepared from [^{14}N]-*p*-nitrophenyl phosphate (^{15}N -depleted)

- (16) Humphry, T.; Forconi, M.; Williams, N. H.; Hengge, A. C. *J. Am. Chem. Soc.* **2002**, *124*, 14860–14861.
- (17) Hengge, A. C.; Cleland, W. W. *J. Am. Chem. Soc.* **1990**, *112*, 7421–7422.
- (18) Hengge, A. C.; Edens, W. A.; Elsing, H. *J. Am. Chem. Soc.* **1994**, *116*, 5045–5049.
- (19) O'Leary, M. H.; Marlier, J. F. *J. Am. Chem. Soc.* **1979**, *101*, 3300–3306.
- (20) Hengge, A. C. *Acc. Chem. Res.* **2002**, *35*, 105–112.

with natural abundance oxygen in the bridging position, mixed with complex made from [^{15}N]-*p*-nitrophenyl phosphate and ^{18}O in both bridging positions. The ^{18}O was incorporated from water during the synthesis of the complex, modifying the procedure by using 97% ^{18}O -labeled water and anhydrous $^t\text{BuONa}$ as the base to synthesize the triol-bridged precursor,⁴ and by using anhydrous trifluoromethane sulfonic acid in 97% ^{18}O -labeled water in the complexation step. The level of isotopic labeling at each bridging hydroxide site was determined by electrospray mass spectrometry as $94 \pm 1\%$. The ^{14}N , $^{16}\text{O}_{\text{nucleophile}}$ and the ^{15}N , $^{18}\text{O}_{\text{nucleophile}}$ isotopic isomers were mixed to closely reconstitute the natural abundance of ^{15}N and then used in the $^{18}k_{\text{nuc}}$ KIE determinations.

Kinetic Isotope Effect Determinations. KIE determinations were conducted in triplicate at 25 °C. The dicobalt–phosphate ester complex (80 mg) was dissolved in 40 mL of 20 mM acetate buffer, pH 4.0. To initiate the reaction, the pH was quickly raised to 7.0 by adding an aliquot of 400 mM HEPES buffer, pH 9.0. After approximately one half-life (~ 200 s for **1**, ~ 3 h for **2**), the reaction was swiftly stopped by the addition of an aliquot of 1 N HCl to return the pH of the solution to 4.0.

The progress of the reaction at this point was determined by measuring the absorption at 400 nm of two aliquots from the reaction mixture. Immediately after the reaction was stopped, one 500 μL aliquot of the reaction mixture was added to 3 mL of 0.1 N NaOH and another 500 μL aliquot was added to 3 mL pH 4 acetate buffer. The aliquot in NaOH is quickly hydrolyzed to completion, and served as a total hydrolysis reference to the partial hydrolysis aliquot in acetate. The concentration of nitrophenol in each aliquot was determined from the absorbance at 400 nm of a 50 μL sample added to a cuvette containing 3 mL of buffer at pH 6.5. The ratio of the two absorbances gives the fractional progress of the reaction when it was stopped.

The nitrophenol product was separated from the unreacted substrate by three successive extractions with a like volume of ether at pH 4. The pH of the solution containing the residual (unreacted) complex was then raised back to pH 7.00 and stirred for ~ 20 half-lives. After titration back to pH 4.0, the nitrophenol liberated from the residual complex was then extracted in the same manner.

The ether fractions were dried over magnesium sulfate and filtered, and the solvent was removed by rotary evaporation. The *p*-nitrophenol samples were sublimed under vacuum at 90 °C, and 1.0–1.5 mg samples were prepared for isotopic analysis on an ANCA-NT combustion system in tandem with a Europa 20-20 isotope ratio mass spectrometer.

The $^{15}\text{N}/^{14}\text{N}$ ratios were measured for the product (R_p) and of the remaining starting material (R_s) at partial reaction, as well as in the original mixture (R_o), the latter by analyzing nitrophenol liberated after a sample of the original complex was allowed to react to completion. The isotope effects were calculated using eqs 1 and 2.²¹

$$\text{isotope effect} = \log(1 - f) / \log[(1 - f)(R_s/R_o)] \quad (1)$$

$$\text{isotope effect} = \log(1 - f) / \log(1 - f(R_p/R_o)) \quad (2)$$

For each isotope effect the values calculated from R_o and R_s (eq 1) and from R_o and R_p (eq 2) agreed within experimental error and were averaged to give the final result. The ^{15}N KIE is given directly from these equations. In the ^{18}k isotope effect experiments, the observed KIEs given by the above equations were corrected for the ^{15}k isotope effect, and for incomplete levels of isotopic incorporation. The derivations of the equations used for these corrections in experiments with one ^{18}O label ($^{18}k_{\text{lg}}$) and for experiments with two labels ($^{18}k_{\text{nuc}}$) have been described.²² The equations, and the levels of isotopic incorporation of each of the isotopic isomers, are given in Supporting Information.

(21) Bigeleisen, J.; Wolfsberg, M. *Adv. Chem. Phys.* **1958**, *1*, 15–76.

(22) Hermes, J. D.; Morriscal, S. W.; O'Leary, M. H.; Cleland, W. W. *Biochemistry* **1984**, *23*, 5479–5488.

Table 1. KIE Results from **1** and **2**, and Additional KIEs for Comparison

isotope effect	monoester complex 1	diester complex 2 ¹⁶	4-nitrophenyl phosphate monoester ¹⁸	4-nitrophenyl phosphate diesters ^{10,20}
^{15}k	1.0011(4)	1.0026(2)	1.0028(2)	1.0007–1.0016
$^{18}k_{\text{lg}}$	1.019(1)	1.029(2)	1.0189(5)	1.0042–1.0063
$^{18}k_{\text{nuc}}$	1.013(1)	0.934(2)	na	1.027(1)

Results and Discussion

Table 1 shows the KIE results for the hydrolysis of **1**. For purposes of comparison, we also include in the table previously reported data for the complexed diester **2**, the data for the uncatalyzed hydrolysis of uncomplexed *p*-nitrophenyl phosphate dianion, and the range of values for the hydrolysis of several uncomplexed phosphate diesters with the *p*-nitrophenol leaving group. The diester nucleophile KIE is that for the alkaline hydrolysis of thymidine-5'-*p*-nitrophenyl phosphate.¹⁰ The standard errors in the last decimal places are shown in parentheses.

The rates of reaction of the uncatalyzed monoester and diesters required that their KIEs be measured at 95 and 100 °C, respectively. This contrasts to the 25 °C reaction temperature used when measuring the KIE values from the reactions of **1** and **2**. The difference in temperatures requires a reduction of approximately 20% to be applied to the KIEs obtained at higher temperatures for proper comparison. However, this correction is not large enough to affect the present discussion.

The observed kinetic isotope effects reflect both the fractionation of the isotopes for equilibria before formation of the transition state, and the kinetic isotope effect on the rate-limiting step. The KIE, in turn, is composed of two factors, the temperature-independent factor (TIF) and the temperature-dependent factor (TDF). The TIF, or the imaginary frequency factor, reflects the extent to which the isotopically labeled atom participates in reaction coordinate motion. This factor always favors the lighter isotope, since the frequency that is lost is larger for the lighter isotope, producing a normal contribution to the observed isotope effect.²³ The TDF reflects differences in bonding of the labeled atom in the ground state compared to the transition state. Tighter or “stiffer” bonding to the labeled atom favors the heavier isotope and results in an inverse isotope effect, while “looser” bonding yields a normal isotope effect.

Nucleophile KIEs are generally normal, because the normal contribution from the TIF usually outweighs the inverse contribution that arises from bond formation.^{10,24,25} Inverse nucleophile KIEs are possible in late transition states where bond formation is so advanced that the inverse contribution from the TDF outweighs the TIF.^{25,26} An observed nucleophile isotope effect may also be inverse in a stepwise mechanism in which nucleophilic attack forms an intermediate, when the subsequent breakdown of the intermediate is rate-determining. In such a

(23) Melander, L.; Saunders, W. H. *Reaction Rates of Isotopic Molecules*; Wiley: New York, 1980; pp 152–154.

(24) Westaway, K. C.; Fang, Y.; Persson, J.; Matsson, O. *J. Am. Chem. Soc.* **1998**, *120*, 3340–3344. Lynn, K. R.; Yankwich, P. E. *J. Am. Chem. Soc.* **1961**, *83*, 53–57. Ando, T.; Yamataka, H.; Wada, E. *Isr. J. Chem.* **1985**, *26*, 354–356. Marlier, J. F.; Dopke, N. C.; Johnstone, K. R.; Wirdzig, T. *J. Am. Chem. Soc.* **1999**, *121*, 4356–4363.

(25) Paneth, P.; O'Leary, M. H. *J. Am. Chem. Soc.* **1991**, *113*, 1691–1693.

(26) Hogg, J. L.; Rodgers, J.; Kovach, I.; Schowen, R. L. *J. Am. Chem. Soc.* **1980**, *102*, 79–85.

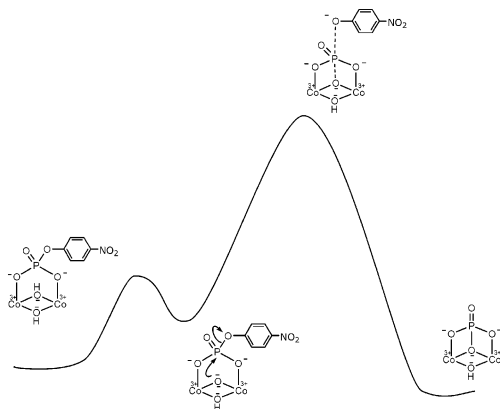


Figure 4. Proposed mechanism of hydrolysis for the monoester complex **1**.

mechanism, the observed nucleophile KIE represents the equilibrium isotope effect on formation of the intermediate.¹⁶

Monoester Complex 1. The most significant difference in the data for the monoester and diester complexes is the normal nucleophile KIE for the reaction of **1**, in contrast to the inverse value for the reaction of **2**. As discussed above, the observed $^{18}k_{\text{nuc}}$ of 1.013 will have contributions from equilibrium deprotonation to form the nucleophilic bridging oxo species, and from the KIE arising from the transition state for nucleophilic attack. There are no EIE values in the literature for deprotonation of hydroxide to form oxide. The ^{18}K EIE for deprotonation of water to form hydroxide is 1.04,²⁷ but this value is elevated by contributions from the first-sphere water molecules that are hydrogen bond donors. The EIE is sharply reduced to 1.012 for deprotonation of a water molecule coordinated to a single Co(III) ion, a value obtained from the EIEs between $(\text{NH}_3)_5\text{Co(III)}\text{-OH}_2$ and water (1.0196) and between $(\text{NH}_3)_5\text{Co(III)}\text{-OH}$ and water (1.008).²⁸ It seems a logical expectation that coordination to a second Co(III) should reduce this fractionation factor still further. The force constant for the coordination of oxygen to the metal ions will be greater for hydroxide than for water, and, in turn, greater for the oxide than for hydroxide. Thus, the fractionation associated with loss of the proton is partly compensated for by enhanced fractionation exerted by the Co(III) ions. While these literature values are for the deprotonation of water to form hydroxide, and not for deprotonation of hydroxide to form the oxide that occurs in the reactions of **1** and **2**, these are the closest models available. We conclude that the normal EIE for deprotonation of the bridging hydroxide to the nucleophilic oxide is smaller than the observed $^{18}k_{\text{nuc}}$ of 1.013, perhaps significantly so. We thus conclude that the kinetic component of $^{18}k_{\text{nuc}}$ is normal, with an upper limit of 1.013.

The normal nucleophile KIE for the reaction of **1** indicates that bond formation occurs in the rate-limiting step. The combination of significant KIEs for both the nucleophile and leaving group indicate that bond formation and bond fission occur in the same step, in a concerted mechanism for phosphoryl transfer, illustrated in Figure 4. This scheme shows the initial deprotonation to form the bridging oxo species, which previous studies show is the nucleophile.³ The nucleophile KIE for the reaction of **1** is only half as large as that reported for the alkaline hydrolysis of the diester thymidine-5'-*p*-nitrophenyl phosphate.¹⁰

This might be taken as an indication of greater bond formation in the transition state of the hydrolysis of **1** than the hydrolysis of thymidine-5'-*p*-nitrophenyl phosphate (recall that nucleophile KIEs are larger for early transition states, becoming smaller as the fraction of bond formation increases). However, differences between the nucleophiles preclude a direct comparison. As the nucleophile bond forms in the reaction of **1**, the bridging oxide may well experience greater stiffening of vibrational frequencies than uncomplexed hydroxide, which might cause the nucleophile KIE for **1** to move more rapidly in the inverse direction as a function of bond formation. Nonetheless, the nucleophile isotope effect indicates a considerable degree of bond formation in the transition state. This is in contrast to the minimal degree of nucleophilic participation thought to occur in the reaction of the uncomplexed monoester dianion implied from linear free energy relationships.²⁹

The $^{18}k_{\text{lg}}$ isotope effect for the reaction of **1** is the same as that for the hydrolysis of uncomplexed *p*NPP dianion at 95 °C. Since the latter KIE is suppressed somewhat by the elevated temperature, this indicates a slightly smaller degree of P–O bond fission in the reaction of **1**. Yet, the ^{15}k suggests that less than half as much delocalized charge resides on the leaving group in the transition state of the reaction of **1**. In the transition state for hydrolysis of uncomplexed *p*NPP, the leaving group is in close proximity to the anionic phosphoryl group. This will increase the degree of charge delocalization (the transition state is late and the leaving group bears close to a full charge). This is thought to account for the observation that the ^{15}k for *p*NPP hydrolysis (1.0028 ± 0.0002) is larger than the ^{15}k for deprotonation (1.0023 ± 0.0001). In the reaction of **1**, the negative charge on the phosphoryl group is partially neutralized as a result of complexation to the two Co(III) ions, evidently lessening charge repulsion and resulting in less delocalization into the aromatic ring.

The previously reported Brønsted slope for the reaction of **1** is large (-1.102).³ Consideration of the β_{eq} led to an estimate of two-thirds bond cleavage in the transition state. The maximum for the $^{18}k_{\text{lg}}$ with the *p*-nitrophenol leaving group at 25 °C is ~ 1.030 ,²⁰ and thus the measured value of 1.019 is consistent with this estimation.

Diester Complex. As is the case with **1**, reaction of the diester complex **2** involves equilibrium deprotonation of a bridging hydroxide followed by nucleophilic attack at phosphorus.^{4,30}

The large inverse nucleophile KIE for the reaction of diester complex **2** led to the conclusion that reaction takes place via a two-step addition–elimination mechanism, as shown in Figure 5.¹⁶ In this mechanism, nucleophilic addition occurs before rate-limiting expulsion of the leaving group. In such a mechanism there is no normal imaginary frequency factor since this bond is fully formed before the transition state of the rate-limiting step. In contrast to KIEs, inverse EIEs are common. For example, the fractionation factor between water and the alcohol of malate is 0.968 in the direction from water to malate,³¹ as a hydrogen atom is replaced by a larger group, introducing new vibrational modes. The even more inverse isotope effect observed in the reaction of **2** likely results from the highly constrained situation of the oxygen atom in the intermediate **B**.

(29) Kirby, A. J.; Jencks, W. P. *J. Am. Chem. Soc.* **1965**, *87*, 3209–3216.

(30) Wahnon, D.; Lebus, A.-M.; Chin, J. *Angew. Chem., Int. Ed. Engl.* **1995**, *34*, 2412–2414.

(31) Blanchard, J. S.; Cleland, W. W. *Biochemistry* **1980**, *19*, 4506–4513.

(27) Green, H.; Taube, H. *J. Phys. Chem.* **1963**, *67*, 1565–1566.

(28) Hunt, H. R.; Taube, H. *J. Phys. Chem.* **1959**, *63*, 124–125.

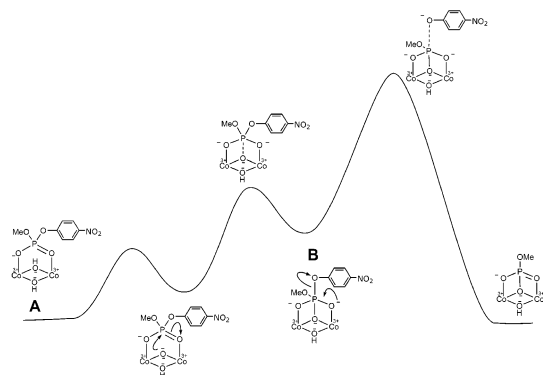


Figure 5. Proposed mechanism of hydrolysis for the diester complex **2**.

The leaving group is then expelled in the rate-limiting breakdown of this intermediate.

The β_{lg} of -1.38^4 is much larger than for the alkaline hydrolysis of uncoordinated phosphodiester ($\beta_{lg} = -0.64$).³² An estimation⁴ of β_{cql} suggests that leaving group bond fission in the hydrolysis of **2** is about twice as advanced in the transition state as for uncomplexed diesters. Consistent with the Brønsted data, the $^{18}k_{lg}$ indicates much greater P–O bond fission to the leaving group in the transition state of the hydrolysis of diester complex **2** than in the hydrolysis of uncomplexed alkyl-*p*-nitrophenyl phosphodiester, and the ^{15}k indicates more negative charge on the leaving group. The LFER and the KIE data show that in this transition state, the P–O bond is substantially broken, and there is essentially a full negative charge on the departing nitrophenolate.

This points to a very different mechanism at work in the hydrolysis of the complexed diester **2** than in the alkaline hydrolysis of uncomplexed diesters. There is also a significant

difference between the mechanisms of the monoester and diester complexes **1** and **2**.

Comparing Transition States. The mechanisms of the reactions of complexes **1** and **2**, and of the thymidine-*p*-nitrophenyl phosphate, are shown on a More-O’Ferrall–Jencks diagram in Figure 6. Complex **1** and uncomplexed diesters are both proposed to have $A_N D_N$ mechanisms. Complexed diester **2** most likely reacts via an addition–elimination ($A_N + D_N$) mechanism, in contrast to the concerted mechanism of uncomplexed diesters. Complexation of the monoester results in a transition state with considerably more nucleophilic participation, and a slightly smaller degree of P–O bond fission, than in reactions of uncomplexed *p*NPP, but the reaction remains concerted.

Charge Balance. Why do the two dicobalt complexes, monoester and diester, proceed by different mechanisms? Momentarily excluding Lewis acid activation, simple charge balance considerations of the cobalt centers may also play a role in determining the mechanisms of hydrolysis of **1** and **2**. Sykes has demonstrated that a dicobalt center approximates a single proton in terms of charge balance.³³ If this is the case, the coordinated diester substrate bears approximately zero net negative charge on the phosphoryl group. By the same accounting, the coordinated monoester substrate will bear approximately one negative charge. It has previously been proposed that phosphoryl transfer reactions follow a tendency for the phosphoryl group to bear a charge of about -1 in the transition state.¹² Thus, uncoordinated monoester dianions react by a loose transition state in which the dinegative phosphoryl group of the reactant sheds nearly a full negative charge to the leaving group in a late transition state. Diesters have roughly synchronous transition states in which they maintain a uninegative charge,

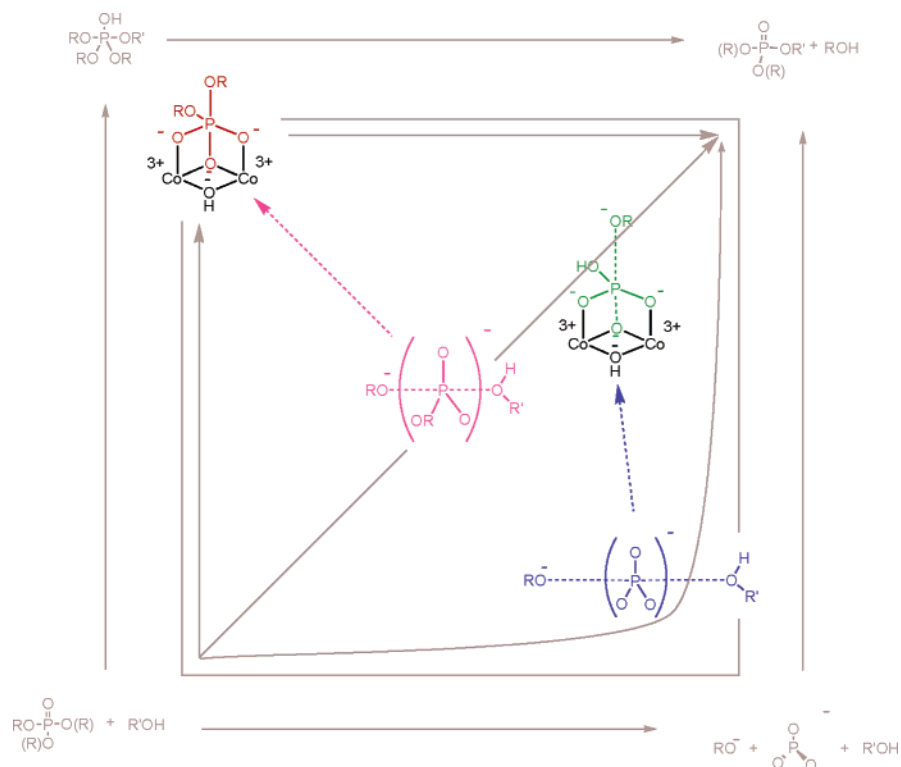


Figure 6. A More-O’Ferrall–Jencks diagram showing the mechanistic changes that occur upon complexation to the dicobalt center of *p*-nitrophenyl phosphate (looser blue to tighter green) and ethyl-*p*-nitrophenyl phosphate (pink transition state to red intermediate). In gray are shown the limiting hydrolysis mechanisms from Figure 2.

and neutral triesters react by more associative transition states, in which the phosphoryl accepts negative charge. In the diester complex **1**, the phosphoryl group is essentially neutral and can accept a full negative charge from the nucleophile in the first step of a two-step mechanism. The phosphate monoester, formally a dianion but effectively a monoanion in the complex, loses a negative charge at the same time it accepts one, in a concerted mechanism in which bond formation and bond fission are more synchronous than in the hydrolysis of uncomplexed *p*NPP.

Conclusions

The impressive rate enhancement of hydrolysis gained by coordination of a phosphate monoester to two cobalt ions takes place by a reaction that remains concerted, like that of uncomplexed monoester dianions. Greater nucleophilic participation in the transition state of the *p*-nitrophenyl phosphate

complex is implied relative to the transition states of reactions of uncomplexed phosphate monoesters, though the reaction remains concerted. In contrast, coordination of a diester to the complex results in a change from a concerted reaction to a two-step, addition–elimination pathway. Assuming that coordination to the complex approximates a single proton in terms of overall charge balance, the resulting complexes seem to obey the trend for phosphoryl groups to bear close to a unit negative charge in their transition states.

Acknowledgment. The authors thank the NIH for financial support (GM47297 to A.C.H.) and the BBSRC/EPSRC for a studentship (to M.F.).

Supporting Information Available: Equations used to obtain the ¹⁸O isotope effects from the observed isotope effects, and the levels of isotopic incorporation of each of the isotopic isomers. This information is available free of charge via the Internet at <http://pubs.acs.org>.

JA047110G

(32) Kirby, A. J.; Younas, M. *J. Chem. Soc. (B)* **1970**, 510–513.

(33) Edwards, J. D.; Foong, S.-W.; Sykes, A. G. *J. Chem. Soc., Dalton Trans.* **1973**, 829–838.